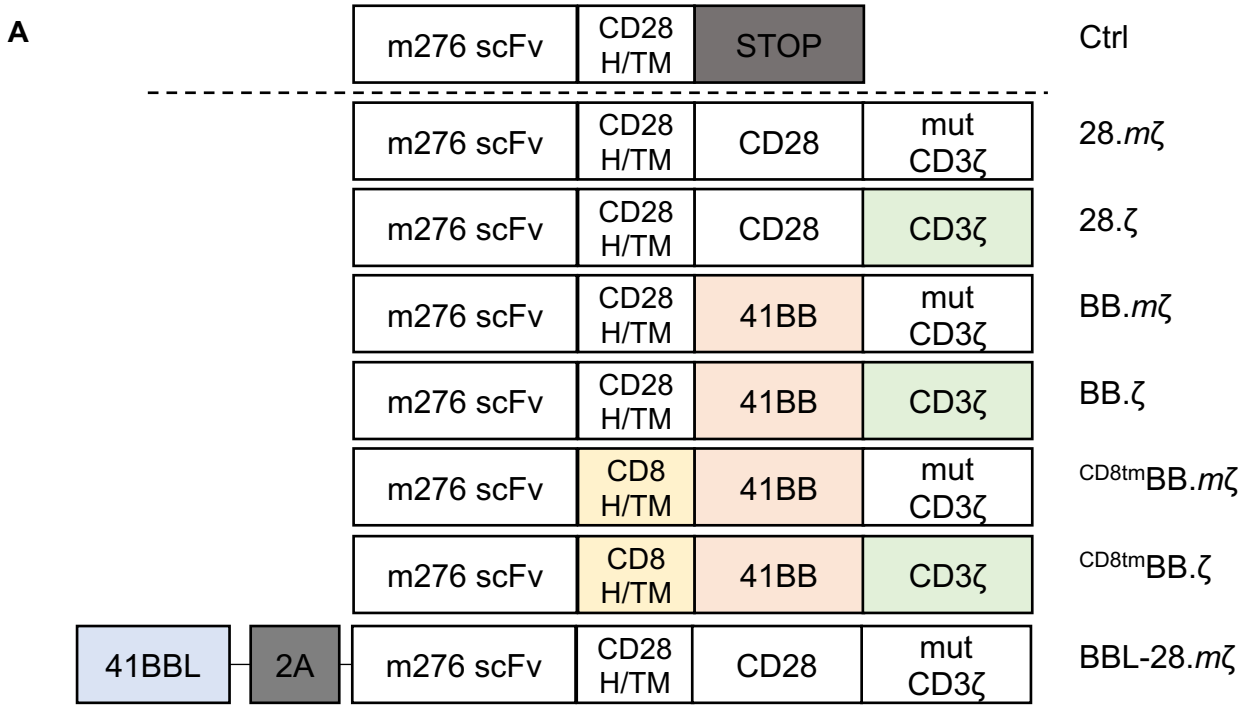

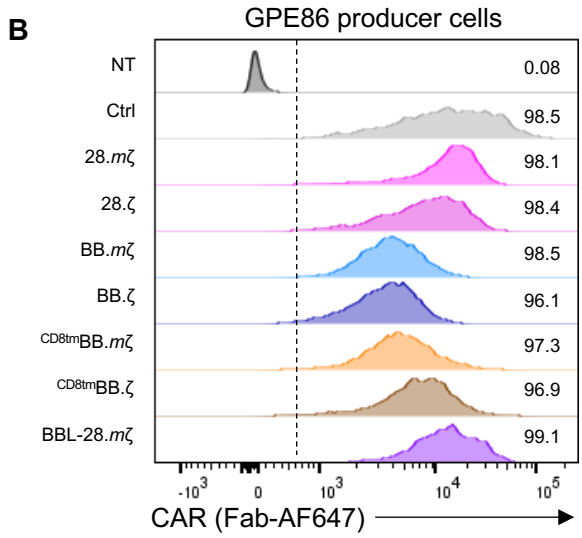

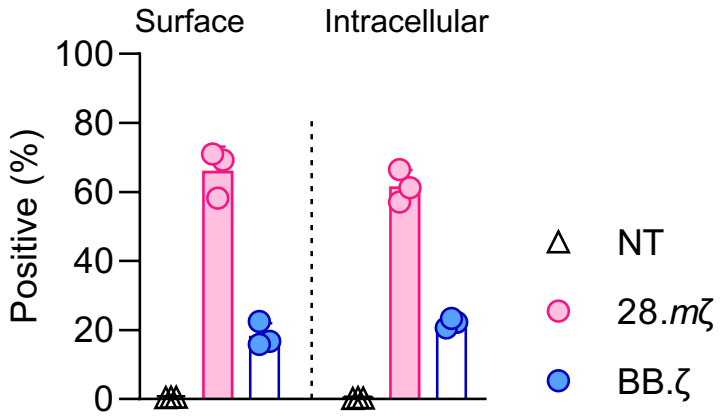

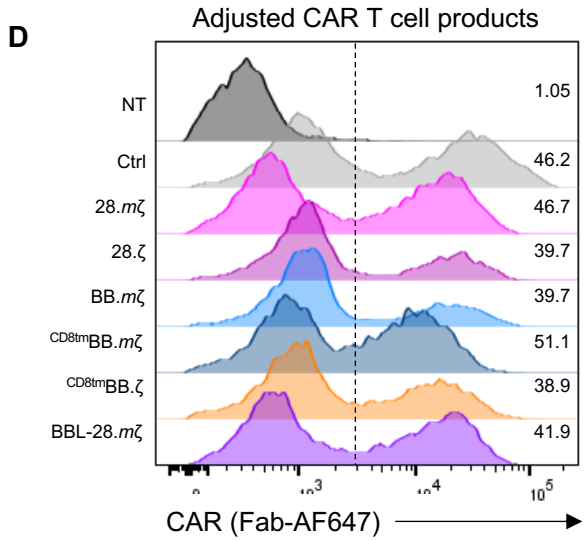

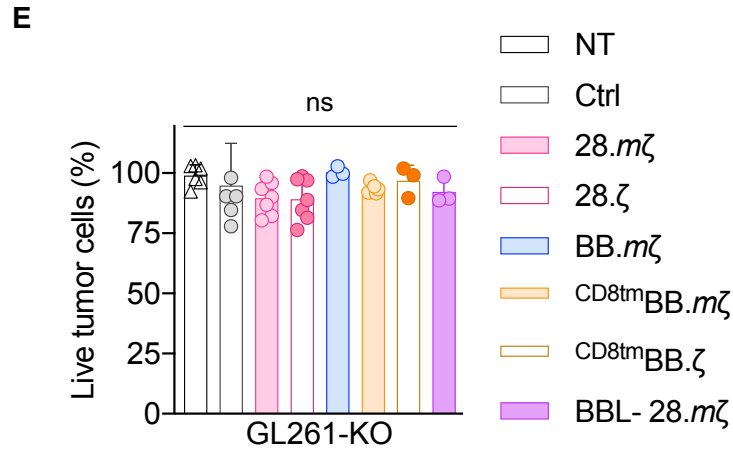

Supplemental Figure 1

Supplementary Figure 1: Generating a library of syngeneic B7-H3 CARs with different transmembrane, costimulatory, and activation domains. **(A)** Scheme of mB7-H3-CAR constructs. **(B)** Representative flow plots of GPE-86 producer cell lines expressing different CAR constructs post FACS sorting for the top positive cells. **(C)** Quantitative bar graph of %F(ab′)2-positive T cells from surface and intracellular staining of B7-H3 CAR T cells expressing 28.*mζ* and BB.ζ CARs. **(D)** Representative flow plots of %F(ab′)2-positive T cells titrated to an average of 40% CAR expression with NT T cells. **(E)** MTS cytotoxicity assay against GL261 *B7h3*-KO tumor cells at an E:T ratio of 4:1 (n = 6, mean ± SD, 2-way ANOVA with Tukey's test for multiple comparisons).

A

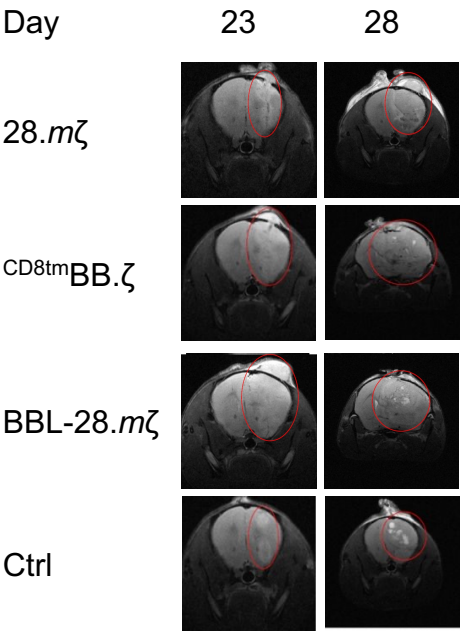

B

1. Enzymatic digestion of tumors (collagenase 1mg/ml; DNase 50 U/ml) → **2. Stain single cells** (CD45; Ter119; TotalSeq-B antibodies) → **3. Sort live CD45+ and CD45- cells** (mix at 70:30 ratio for scRNAseq)

C

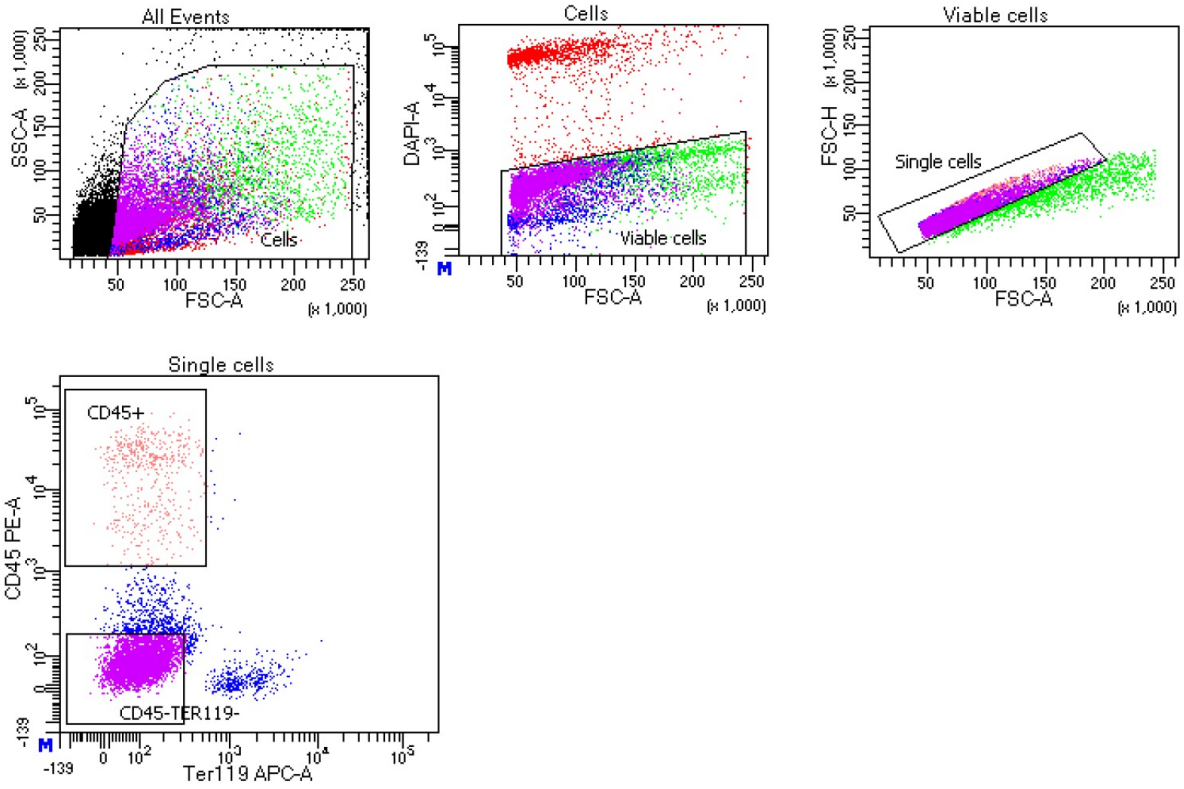

Supplemental Figure 2

Supplementary Figure 2: Experimental set-up of single cell RNAseq experiments for gene expression analyses early after CAR T cell injection. **(A)** Representative images from axial brain MRI before CAR T cell treatment at day 23 post-tumor implantation and right before brain tissue harvesting at day 28 post-tumor implantation. **(B)** Experimental scheme for processing brain tissues for single cell RNAseq. **(C)** Representative flow plot from FACS sorting and gating scheme showing the two viable populations sorted for sequencing analysis ((i) Live, TER119-, CD45+ and (ii) Live, TER119-, CD45-). Samples i and ii were mixed at 70:30 ratio prior to loading on chromium controllers.

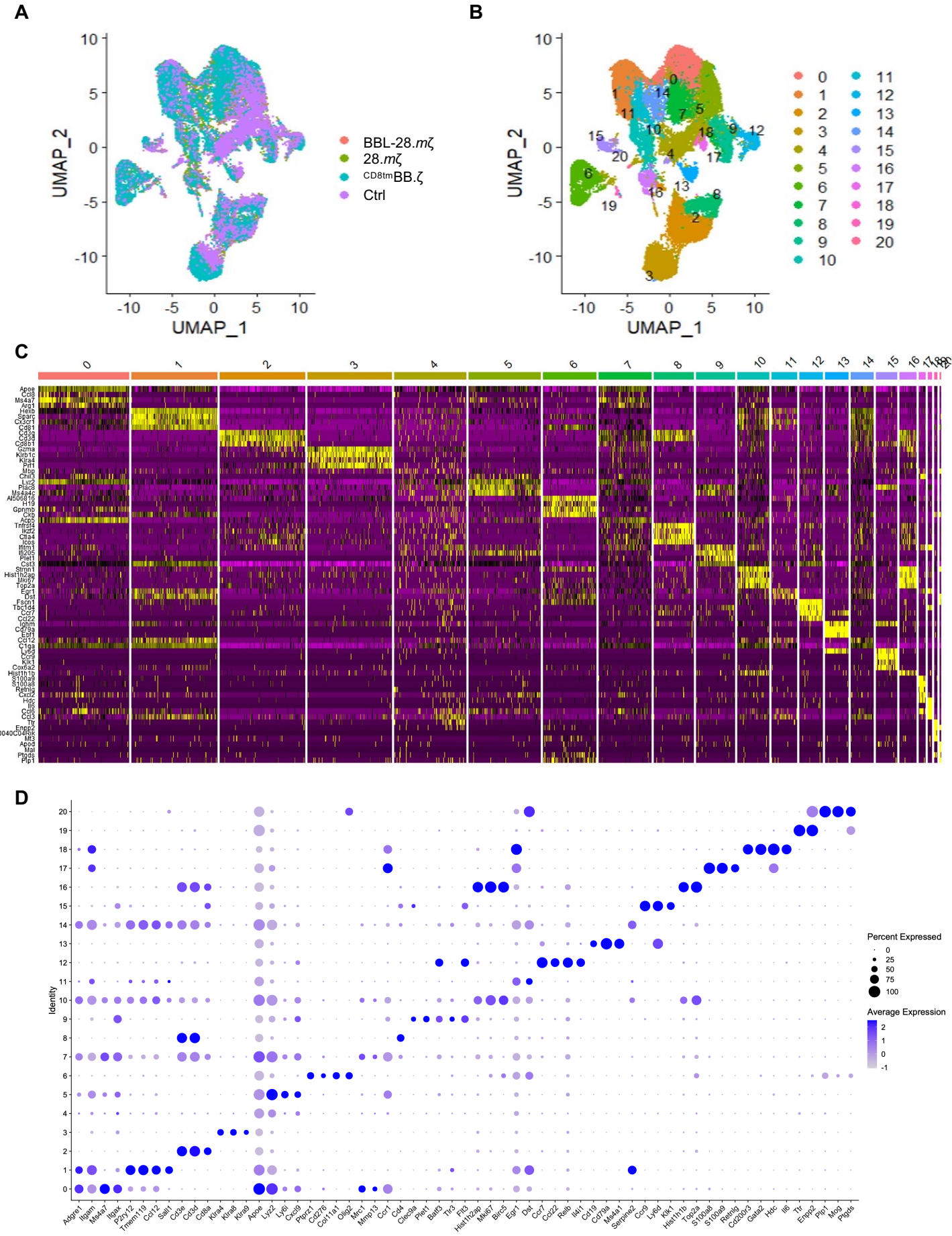

Supplemental Figure 3

Supplementary Figure 3: Analysis of single cell RNA-seq data using 10 dimensionality reduction method. **(A)** UMAP visualization of major immune cell clusters per treatment group. **(B)** UMAP plot of single cells from four treatment groups colored by their distribution into 21 major cell types. **(C)** Heatmap of top upregulated genes within the 21 major cell clusters. **(D)** Dot plot visualizing the canonical cell-type marker expression within each cell cluster.

Cluster	Functional group	Subgroup (if any)	Gene Markers
0	Mac-1	Monocyte-derived TAM	*Adgre1, Itgam, Itgax, Itga4 (Ms4a7, Pf4)*
1	MG-1	Brain Microglia	*P2ry12, Tmem119, Ccl12, Sall1*
2	T cells	CD8	*Cd3e, Cd3d, Cd8a*
3	NK cells		*klra4, klra8, klra9*
4	Other	Myeloid/granulocyte	*Mix*
5	Monocytes	Inflammatory	*Ly6i, Cxcl9, Cxcl10, Lyz2*
6	Tumor cells		*Ptprz1, Cd276, Col11a1, Olig2*
7	Mac-2	Monocyte-derived TAM	*Adgre1, Itgam, Itgax, Itga4 (Mrc1, Mmp13, Ccl8, Ifng)*
8	T cells	CD4, Treg	*Cd4, Foxp3*
9	DC-1	cDC1	*Xcr1, Clec9a, Plet1, Tlr3, Batf3, Flt3*
10	MG/Mac-1	proliferative microglia-derived TAM	*Adgre1, Itgam (Birc5, Hist1h2ap, Mki67)*
11	MG-2	Mixed population	*Egr1, Dst, Mef2*
12	DC-2	cDC, migratory	*Ccr7, Ccl22, Relb, Il4i1*
13	B cells		*Cd79a, Cd19, Ms4a1*
14	MG/Mac-2	Inflammatory	*Tmem119, Cxcr1, Serpine2*
15	DC-3	pDCs	*Ccr9, Ly6d, Klk1*
16	T cells	Proliferating	*Hist1h1b, Top2a*
17	Neutrophils		*Ly6g, S100a8, S100a9, Retnlg*
18	Basophils		*Cd200r3, Gata2, Il6*
19	Epithelial/CNS		*Ttr, Enpp2*
20	Fibroblasts	oligodendrocytes	*Plp1, Mog, Ptgds*

Supplementary Figure 4: Manual validation of immune cell clusters from single cell RNA-seq data. Cluster identities were verified by expression of canonical markers for each cell type as well as by manual review of top upregulated genes relevant to the functional pathways within each cluster.
Mac – macrophages, MG – microglia, DC – dendritic cells, CNS – central nervous system

A

T cell cluster	Subgroup	Gene markers
0	Activated/Exhausted CD8 Teff	*Gzma, Nkg7, Klrc1, Prf1, Lag3, Ctla4, Havcr2, Pdcd1, Tox*
1	CD8 Tnaive	*Sell, Tcf7, Lef1*
2	CD4 Treg	*Foxp3, Tnfrsf4, Il2ra*
3	Proliferating CD8 Teff	*Hist1h2ap, Mki67, Top2a*
4	Resting/quiescent T cells (CD4/8 mix)	*Klf2, Tcf7, Slfn1, Klf3*
5	CD8 TRM	*Ly6c2, Xcl1, Cxcr6*
6	Activated/Exhausted TRM (CD4/8 mix)	*Cd69, Cd28, C1qa, Lag3, Ctla4, Havcr2, Tigit*
7	Exhausted CD4 T cells	*Lag3, Ctla4, Havcr2, Pdcd1, Tox*
8	Proliferating CD8 Teff	*Mcm5, Mcm6, Mcm7, Pcna, Ybx3*
9	Gamma-delta T cells	*Trdc, Il17a, Tcrg-C1*
10	Activated CD8 Teff	*C1qa, C1rc, H2-Eb1, Cxcl9*

B

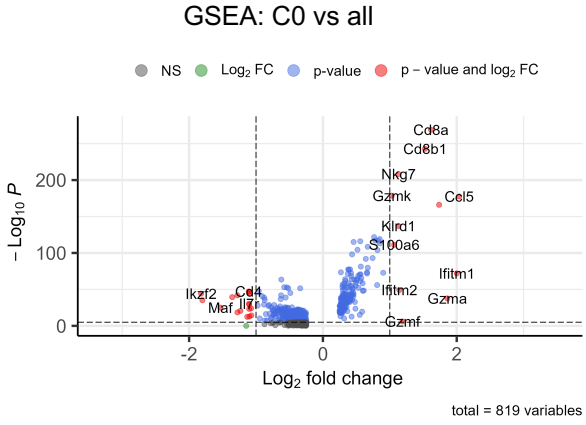

C

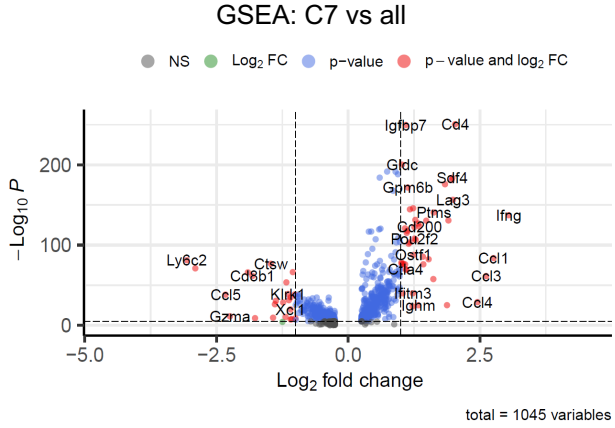

Supplementary Figure 5: Heterogeneity analysis of T-cell responses post CAR T-cell treatment in GL261 glioma bearing mice. Clusters 2, 8, and 16 were re-clustered to further define T-cell populations across treatment groups. **(A)** Table showing top upregulated genes corresponding with the functional phenotype for each of the 10 T-cell subclusters. **(B)** Volcano plot showing the up- and downregulated genes in T-cell subcluster 0 versus all other T-cell subclusters from GSEA analysis. **(C)** Volcano plot depicting the up- and downregulated genes in T-cell subcluster 7 versus all other T-cell subclusters.

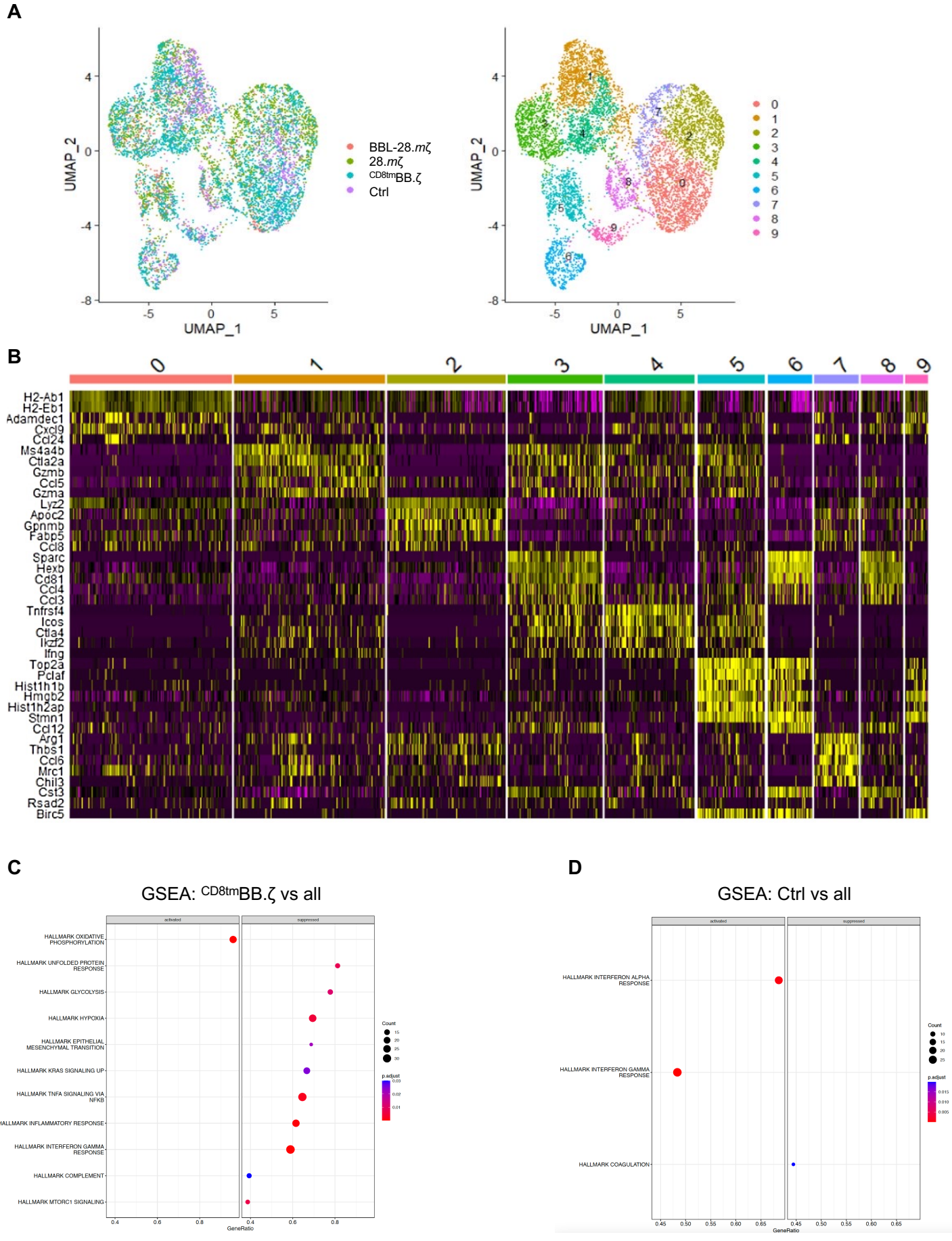

Supplemental Figure 6

Supplementary Figure 6: Heterogeneity analysis of macrophage populations post CAR T-cell treatment in GL261 glioma bearing mice. Clusters 0, 7, 10, and 14 were re-clustered to further define macrophage populations across treatment groups. **(A)** UMAP plot of macrophage subclusters visualized by color according to each treatment group on the left and by each of the 10 major macrophage clusters across the four treatment groups on the right. **(B)** Heatmap showing top upregulated genes within each of the 10 macrophage subclusters. **(C)** GSEA plot depicting the up- and downregulated pathways among macrophage clusters in ^{CD8tm}BB.ζ-CAR treated group versus all. **(D)** GSEA plot depicting the up- and downregulated pathways among macrophage clusters in Ctrl-CAR treated group versus all.

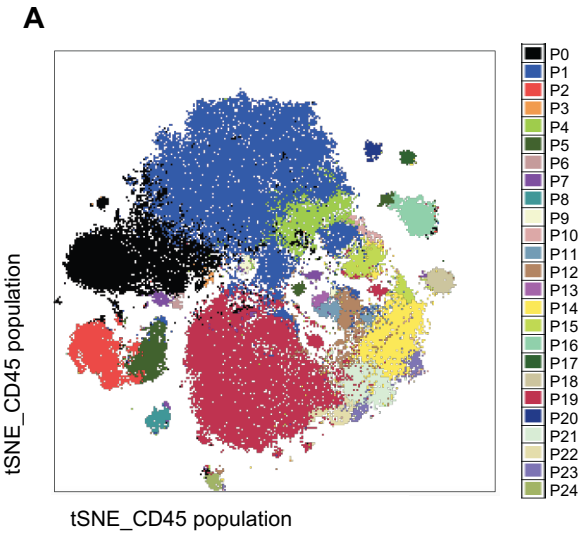

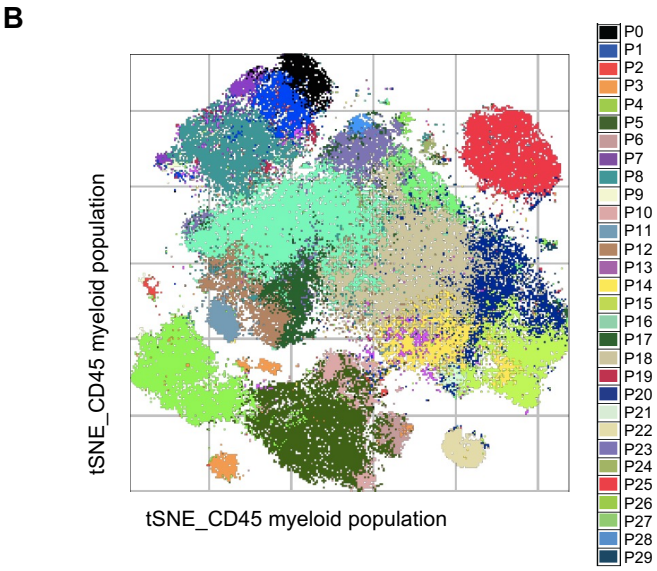

C

Gate: Cell-Sized –> Viable –> Single Cell –> CD45(+)

Cluster	Count	CD11b	NK1.1	CD209a	CD45	CD11c	CD19	F4/80	CD3	CD163	B7-1	Ly6C	CD86	CD64a/b	CD90-1	XCR1	CD123	CD24	CD49b	CD206	Ly6G	MHCII
0	12535																					
1	30166																					
2	4229																					
3	215																					
4	4504																					
5	3186																					
6	275																					
7	809																					
8	919																					
9	517																					
10	498																					
11	725																					
12	2016																					
13	417																					
14	4606																					
15	2233																					
16	2506																					
17	441																					
18	1262																					
19	23735																					
20	590																					
21	3050																					
22	895																					
23	1231																					
24	440																					

D

Gate: Cell-Sized –> Viable –> Single Cell –> CD45(+) –> CD3(-) –> CD19(-) –> CD49b(Lo) –> NK1.1(Lo)

Cluster	Count	CD11b	NK1.1	CD209a	CD11c	F4/80	CD163	B7-1	Ly6C	CD86	CD64a/b	GRP78	XCR1	GFP	CD123	CD24	CD49b	CD206	Ly6G	MHCII
0	2202																			
1	2331																			
2	533																			
3	1587																			
4	9031																			
5	11422																			
6	1459																			
7	1081																			
8	7078																			
9	693																			
10	3590																			
11	1825																			
12	3247																			
13	1429																			
14	3304																			
15	5713																			
16	14354																			
17	4828																			
18	17431																			
19	706																			
20	8562																			
21	1090																			
22	2064																			
23	4883																			
24	668																			
25	8651																			
26	503																			
27	3541																			
28	752																			
29	442																			

Supplemental Figure 7

Supplementary Figure 7: Unsupervised nonlinear dimensionality reduction of flow cytometry data from tumors at endpoint. Detailed information about marker expression patterns in the tumor infiltrates was obtained after T-distributed stochastic neighbor embedding (t-SNE) algorithms were applied with the aid of FlowJo software (Becton Dickenson, San Jose). The identity of each separate cluster in the t-SNE plot was confirmed and further visualized using a FlowSOM heatmap. **(A)** Representative cluster plot of t-SNE mapping to identify the major cell subsets within the CD45+ immune cell population along with the corresponding FlowSOM heatmap for individual markers in **(C)**. **(B)** Representative cluster plot of t-SNE mapping to identify the major myeloid cell subsets by excluding cells positive for all lymphoid markers (CD3, CD4, CD8, CD19, CD49b, and NK1.1) along with the corresponding FlowSOM heatmap in **(D)**.

A

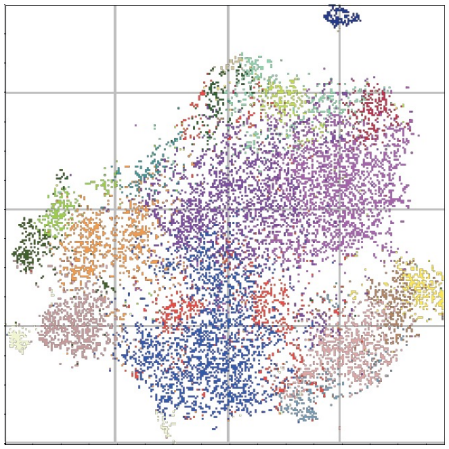

B

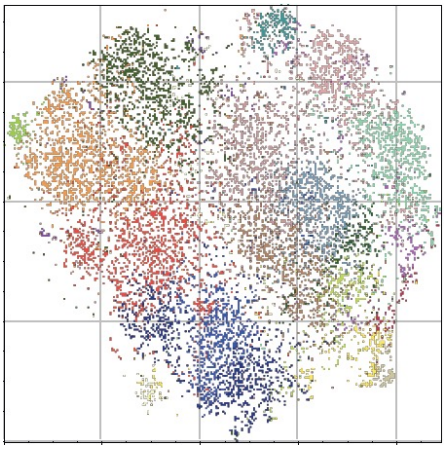

C

Gate: Cell-Sized –> Viable –> Single Cell –> CD45(+) –> CD19(-) –> CD3(+) –> CD4(-) –> CD8(+)

Cluster	Count	B7-H3	CD69	CTLA4	CD103	CD127	CD3	CD49b	CD25	CD62L	CD44	CD90-1	LAG3	CD123	CD8	TIM3	PD1
0	2542																
1	969																
2	1075																
3	310																
4	336																
5	895																
6	2060																
7	207																
8	230																
9	948																
10	310																
11	394																
12	2692																
13	395																
14	338																
15	504																
16	218																
17	62																
18	306																
19	209																

D

Gate: Cell-Sized –> Viable –> Single Cell –> CD45(+) –> CD19(-) –> CD3(+) –> CD8(-) –> CD4(+)

Cluster	Count	B7-H3	CD69	CTLA4	CD103	CD4	CD127	CD3	CD49b	CD25	CD62L	CD44	CD90.1	LAG3	CD123	TIM3	PD1
0	1011																
1	997																
2	1829																
3	1921																
4	162																
5	1405																
6	1230																
7	127																
8	309																
9	276																
10	1025																
11	932																
12	1091																
13	313																
14	373																
15	373																
16	1046																
17	337																
18	124																
19	119																

Supplemental Figure 8

Supplementary Figure 8: FlowSOM combined with t-SNE analysis for CD4 and CD8 T cell populations from tumors at endpoint. **(A)** Representative cluster plot of t-SNE mapping to identify the major cell subsets with the CD8 T cell population along with corresponding FlowSOM heatmap for individual markers in **(C)**. **(B)** Representative cluster plot of t-SNE mapping to identify the major cell subsets of CD4 T cell populations with the corresponding FlowSOM heatmap in **(D)**.

A

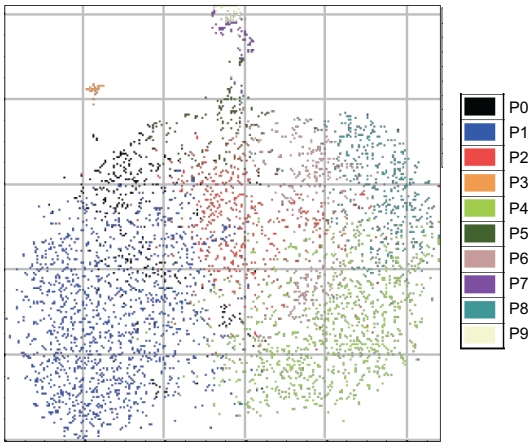

B

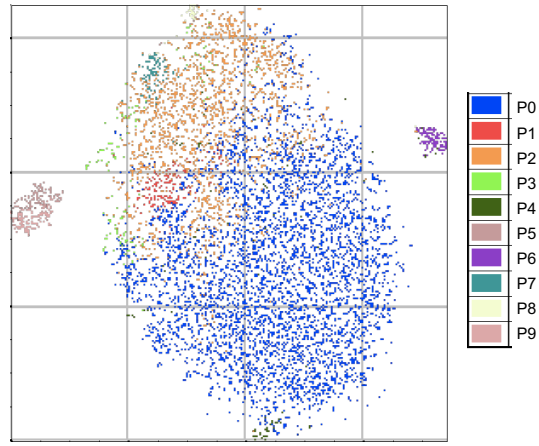

C

Gate: Cell-Sized –> Viable –> Single Cell –> CD45(+) –> B220(-) –> CD3(+) –> TCRb(+) –> CD8(-) –> CD4(+)

Cluster	Count	ARG1	IL17a	CD11c	IFNg	CD4	RORgt	CD25	CD11b	TNFa	F4/80	CD90.1	IL6	AHR	IL10	Foxp3
0	336															
1	1618															
2	502															
3	37															
4	1129															
5	179															
6	378															
7	72															
8	475															
9	74															

Gate: Cell-Sized –> Viable –> Single Cell –> CD45(+) –> B220(-) –> CD3(+) –> TCRb(+) –> CD4(-) –> CD8(+)

D

Cluster	Count	ARG1	IL17a	CD11c	IFNg	RORgt	CD25	CD11b	TNFa	F4/80	CD90.1	CD8a	IL6	AHR	IL10	Foxp3
0	5575															
1	208															
2	2228															
3	188															
4	136															
5	147															
6	168															
7	108															
8	62															
9	180															

Supplemental Figure 9

Supplementary Figure 9: FlowSOM combined with t-SNE analysis for CD4 and CD8 T cell phenotypes from intracellular staining of tumors at endpoint. **(A)** Representative cluster plot of t-SNE mapping to identify the major cell subsets within the CD4 T cell population based on expression of intracellular markers in the FlowSOM heatmap in **(C)**. **(B)** Representative cluster plot of t-SNE mapping to identify the major cell subsets of CD8 T cell population based on intracellular marker expression patterns depicted in the FlowSOM heatmap in **(D)**.

A

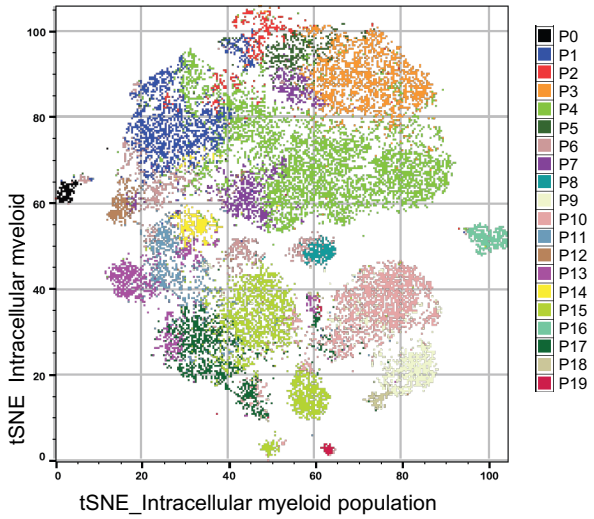

B

Gate: Cell-Sized –> Viable –> Single Cell –> CD45(+) –> CD4(-) –> CD8(-) –> B220(-)

Cluster	Count	ARG1	IL17a	CD11c	IFNg	RORgt	CD25	CD11b	TNFa	F4/80	CD90.1	IL6	AHR	IL10	FoxP3
0	199														
1	1731														
2	468														
3	2184														
4	5939														
5	528														
6	921														
7	1101														
8	383														
9	951														
10	2183														
11	804														
12	369														
13	983														
14	468														
15	2541														
16	450														
17	1518														
18	170														
19	109														

C

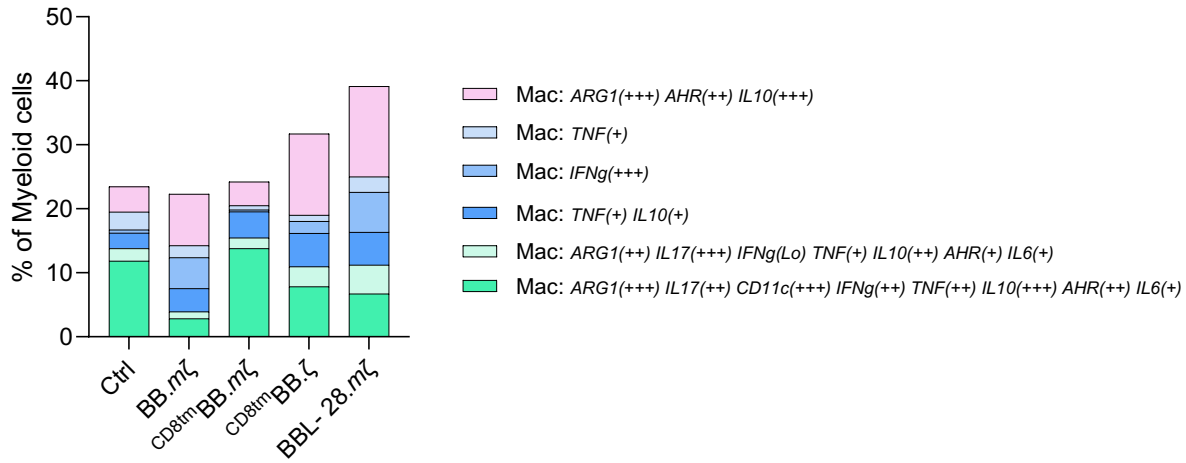

Supplemental Figure 10

Supplementary Figure 10: Unsupervised nonlinear dimensionality reduction of intracellular flow cytometry data from tumors at endpoint. Tumors were permeabilized, fixed, and processed for intracellular staining. Detailed information about surface and intracellular marker expression patterns in the tumor infiltrates was obtained after t-SNE algorithms were applied with the aid of FlowJo software (Becton Dickenson, San Jose). The identity of each separate cluster in the t-SNE plot was confirmed and further visualized using a FlowSOM heatmap. **(A)** Representative cluster plot of t-SNE mapping for myeloid cell subsets stained for intracellular markers along with the corresponding FlowSOM heatmap for individual markers in **(B)**. **(C)** Summary plot of the macrophage/microglia clusters based on their expression of specific intracellular markers. The number of + signs increases with increased MFI for each marker in the relevant cell cluster.